Femtosecond Transition-State Dynamics of Dissociating OCS on the Excited $^1\Sigma^+$ Potential Energy Surface†

Akiyoshi Hishikawa, Kyoko Ohde, Ryuji Itakura, Shilin Liu, and Kaoru Yamanouchi*

Department of Pure and Applied Sciences, College of Arts and Sciences, The University of Tokyo, 3-8-1 Komaba, Meguro-ku, Tokyo 153, Japan

Koichi Yamashita

Department of Applied Chemistry, Graduate School of Engineering, The University of Tokyo, 7-3-1 Hongo, Bunkyo-ku, Tokyo 113, Japan

Received: August 8, 1996⊗

Ultrafast photodissociation dynamics of OCS on the dissociative potential energy surface (PES) of the electronically excited $^1\Sigma^+$ state was investigated by photofragment excitation (PHOFEX) spectroscopy and time-dependent wavepacket calculations. The high-resolution PHOFEX spectrum of the entire $^1\Sigma^+-{}^1\Sigma^+$ transition (63 300−69 350 cm^{-1}) in the vacuum ultraviolet (vacuum UV) region was measured under jet-cooled conditions by using a tunable vacuum UV laser as an excitation light source and by monitoring the fragment S(^{1}S) atom. Due to sufficient vibrational and rotational cooling in a supersonic jet, a simple and distinct vibrational progression of the $^1\Sigma^+-{}^1\Sigma^+$ band was recorded free from vibrational hot bands and the broadening by rotational structure. The autocorrelation function obtained from a Fourier transform of the PHOFEX spectra clearly exhibited recurrences with a period of 42 fs, corresponding to a period of the vibrational motion at the transition state along the direction perpendicular to the dissociation coordinate. This interpretation of the ultrafast motion in the transition-state region was supported by the wavepacket calculation on the *ab initio* PES obtained in the present study, which afforded a period of 48 fs for vibrational motion along the in-phase CO and CS stretching mode at the transition state on the *ab initio* PES. The distinct six peaks broadened due to the fast dissociation process were assigned to the transitions at the v_{TS} = 0−5 levels, where v_{TS} represents a vibrational quantum number for the Feshbach resonances in the in-phase stretching mode at the transition state. For the v_{TS} = 0 peak, the narrowest width corresponding to the lifetime, $\tau(v_{TS})$, of $\tau(0)$ = 133 fs was obtained. It was found that the dissociation lifetime first becomes shorter for a larger v_{TS}, i.e., $\tau(1)$ = 44 fs and $\tau(2)$ = 27 fs, and then, the peak width becomes narrower for the higher vibrational states above v_{TS} = 2, with corresponding lifetimes of $\tau(3)$ = 47 fs and $\tau(4)$ = 44 fs. This deceleration of the dissociation rate for the larger v_{TS} states was interpreted as a result of trapping of a wave function in the in-phase stretching or the CO stretching vibrational motion suppressing the motion along the dissociation coordinate. All six main peaks in the PHOFEX spectra exhibited a characteristic asymmetric profile, originating from the interference between the zero-order discrete states for the in-phase stretching vibration at the transition state and the zero-order continuum states corresponding with the motion along the dissociation coordinate. In the main progression of the PHOFEX spectra, the reversal of the asymmetry direction was also observed. This *q*-reversal phenomenon was ascribed to the characteristic shape of the excited $^1\Sigma^+$ PES near the transition region which causes a phase shift in the wave functions in a narrow energy range.

I. Introduction

The ultrafast dissociation process of small polyatomic molecules initiated by photoabsorption is an important subject in current chemistry.[1,2] The studies on fast photodissociation dynamics in polyatomic molecules have been motivated by a fundamental desire to know how the energy imposed on a molecule evolves among various degrees of freedom, such as electronic, vibrational, rotational, and translational degrees of freedom within a molecule, and how the bond breakage occurs in the course of the intramolecular energy transfer. One of the key words which are crucial to describe photodissociation as well as chemical reaction processes is *a transition state*, which represents a transient molecular configuration located between the reactant and product states with a typical *lifetime* between 100 and 10 fs. The transition state governs the energy flow from the reactants to the products and, thus, plays a central role in determining the characteristic properties of the photodissociation such as dissociation rate and product-state distribution of the photofragments.

In recent years, every effort has been paid to elucidate the dynamics of photodissociating molecules near the transition state. By various laser spectroscopic techniques, the scalar as well as the vector properties of the photofragments have been derived to infer the transition-state dynamics.[2] The recent advent of ultrashort-pulse laser technology has enabled us to probe the ultrafast phenomena near the transition state in a more direct way. Femtosecond spectroscopy has been applied to a variety of molecules and molecular complexes and proved to be a promising technique to study the transition-state dynamics in a real time scale.[1]

On the other hand, as has been discussed by Heller,[3] the essential information about the vibrational dynamics of dis-

* Author to whom correspondence should be addressed.

† Dedicated to Prof. Saburo Nagakura on the occasion of his 75th birthday and retirement from the Graduate University for Advanced Studies, Japan.

⊗ Abstract published in *Advance ACS Abstracts,* December 15, 1996.

S1089-5639(96)02423-1 CCC: $14.00

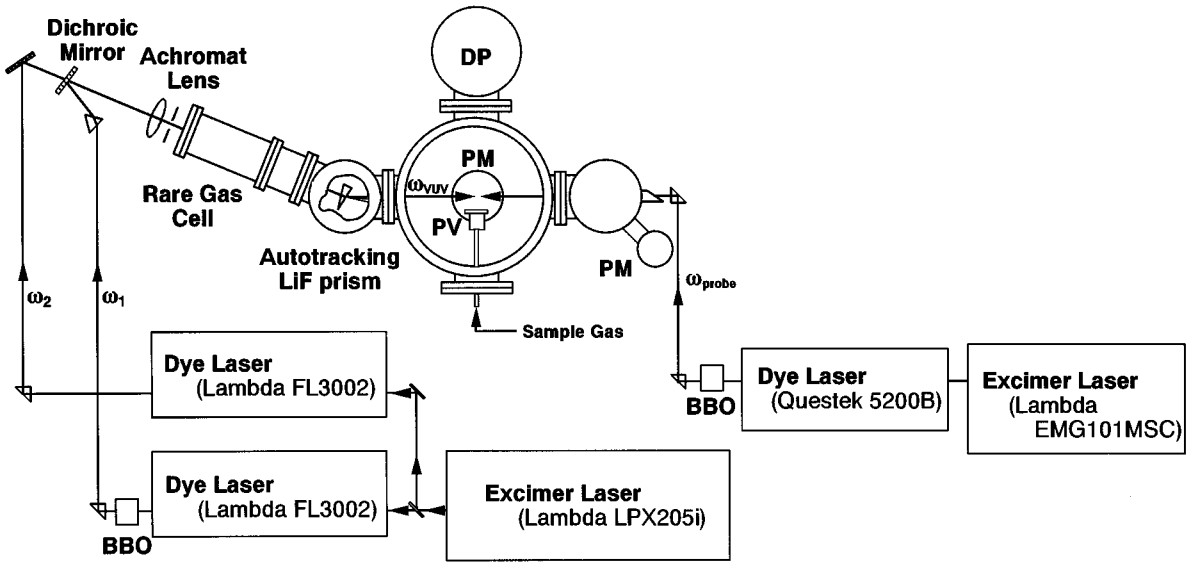

Figure 1. Schematic diagram of the experimental setup for the present vacuum UV PHOFEX measurements.

sociating molecules near the transition state is fully encoded in an optical absorption spectrum. The absorption spectrum in the frequency domain can be translated by the Fourier transformation to the autocorrelation function in the time domain, which describes a periodical motion of the wavepacket on the excited potential energy surface (PES). The Fourier transform analysis of an absorption spectrum has proved to be a powerful method to extract the dynamical information of the system.[2] As has been clearly shown for CO_2 by Schinke and Engel,[4] peaks in the autocorrelation function can be closely related to periods of classical unstable periodic orbits on the dissociative PES. An application of the Fourier transform analysis to the Hartly band of ozone by Johnson and Kinsey[5] demonstrated that small oscillatory structures built on a broad absorption feature contain the information of the classical trajectories of the vibrational motion at the transition state on the PES, leading to a unimolecular dissociation.

A clearer understanding of such dynamics near the transition state from an experimental autocorrelation function has often been provided by theoretical time-dependent wavepacket calculations.[2] The energy flow among the various degrees of freedom in the course of the photodissociation is expressed in this method as the time evolution of a wavepacket on the multidimensional excited-state PES. For instance, the oscillatory structure observed in the Hartly band of ozone has been satisfactorily reproduced recently[6] by 3D wavepacket calculations on an *ab initio* PES, revealing the quantum mechanical origin of the oscillatory structure as the Feshbach-type resonances.

Optical absorption spectra of simple polyatomic molecules often exhibit broadened vibrational band profiles, especially in the vacuum ultraviolet (vacuum UV) wavelength region.[7] As explained above, such spectra in the vacuum UV region should contain valuable information about a very fast photodissociation process occurring in the excited-state PES on a subpico- to femtosecond order, and thus, the molecules are considered to be promoted directly to the transition-state region for unimolecular reaction by photoabsorption. However, in the previous photodissociation studies in the vacuum UV region, laser spectroscopy has provided only fragmental information at fixed wavelengths such as 157 and 193 nm, and until very recently, little effort has been paid to record a high-resolution absorption spectrum in the vacuum UV region, to extract rich and precise information about the dissociation dynamics. We recently focused our attention on the distinct and simple vibrational progression in the $^1\Sigma^+-{}^1\Sigma^+$ absorption band of OCS in the deep vacuum UV region.[8−11] By employing photofragment excitation (PHOFEX) spectroscopy combined with a tunable vacuum UV laser and a supersonic-jet-cooling technique, we demonstrated that the spectrum corresponding with the high-resolution absorption spectrum could be measured under ultracold conditions.

From the Fourier transform of the absorption spectrum of OCS measured by McCarthy and Vaida,[12] we obtained the vibrational period of 41 fs and regarded the period as that of a characteristic vibrational motion along the unstable periodic orbit near the transition-state region.[9] Furthermore, on the basis of the profiles and widths of the transition peaks in the PHOFEX spectrum covering the lower half region of the $^1\Sigma^+-{}^1\Sigma^+$ band, which were measured free from vibrational and rotational congestion, state-specific dissociation processes have been discussed.[10,11]

In our previous studies, the PHOFEX measurements was restricted to the three low-lying peaks in the lower half region of the $^1\Sigma^+-{}^1\Sigma^+$ band. In the present study, we extended the PHOFEX measurements toward the higher energy region to cover the entire $^1\Sigma^+-{}^1\Sigma^+$ band (63 300−69 350 cm^{-1}) to obtained more complete experimental information regarding the photodissociation dynamics. We also derived the PES of the mostly repulsive $^1\Sigma^+$ state from an *ab initio* calculation and performed a wavepacket calculation on the obtained PES in order to identify the transition-state vibrational motion with the 41-fs period. By combining the new experimental and theoretical results, we drew a consistent picture of characteristic vibrational dynamics of OCS, forming the well-isolated vibrational Feshbach resonances in the transition-state region.

II. Experimental Section

The experimental setup used in the present work is shown in Figure 1. The coherent vacuum UV light to photolyze the OCS molecule was generated through the two-photon resonant four-wave difference frequency mixing technique.[13] In order to cover the wide energy range (144−158 nm) of the photolysis light, two different nonlinear media, Xe and Kr, were used for the wavelength region between 150.1 and 158.0 nm and between 144.2 and 149.9 nm, respectively. Two tunable dye lasers (Lambda Physik FL3002) were simultaneously pumped by an excimer laser (Lambda Physik LPX205i). The frequency-doubled output (ω_1) of the first dye laser was tuned to the two-

photon resonance to the Xe $6p[1/2]_0$ (80 119.474 cm^{-1}) or the Kr $5p[1/2]_0$ (94 093.662 cm^{-1}) level, while the wavelength of the second dye laser, whose wavenumber is denoted as ω_2, was scanned between 595 and 738 nm for Xe and between 365 and 404 nm for Kr, respectively. The two laser beams were overlapped colinearly by a dichroic mirror and focused with an achromat lens ($f = 300$) into a stainless steel cell containing the nonlinear medium. The generated coherent vacuum UV light was collimated by an LiF lens, separated from the ω_1 and ω_2 light beams by an LiF prism, and led to a vacuum chamber, where the vacuum UV light beam crossed a pulsed free-jet expansion of sample gas (OCS (7%)/Ar with 1.5 atm of stagnation pressure) 8-mm downstream from the nozzle orifice.

The fragment $S(^1S)$ atom was probed by the laser-induced fluorescence (LIF) in the following scheme:

$$OCS + h\nu\ (144-158\ nm) \rightarrow CO(X^1\Sigma^+) + S\ (^1S) \quad (1)$$

$$S(^1S) + h\nu\ (219\ nm) \rightarrow S(^3D_1{}^o) \quad (2)$$

$$S(^3D_1{}^o) \rightarrow S(^3P) + h\nu\ (148\ nm) \quad (3)$$

Since the photodissociation of OCS in the 140−160-nm region produces the $S(^1S)$ atom with high absolute quantum yield (0.8−1.0),[14] the PHOFEX spectra obtained by probing $S(^1S)$ atoms are expected to be very close to the absorption spectra.

For the probe light, the frequency-doubled output of a dye laser (Questek 5200B), which was pumped by another excimer laser (Lambda Physik EMG101MSG), was used. The delay between the photolysis light and the probe light was controlled by a digital delay generator (Stanford DG535) and was fixed to 0.2−0.3 μs. The delay was sufficiently large to eliminate the weak fluorescence of a trace amount of CO contained in the OCS sample (Matheson, 97.5% purity). The probe laser was mildly focused by a quartz lens ($f = 800$) and introduced into the chamber colinearly with the vacuum UV light in the counterpropagating direction. The profile of the probe laser at the crossing region with the jet expansion was rectangular (1 × 3 mm), with its longer side along the jet axis. This profile of the probe laser assured the spatial overlap between the probe and photolysis laser beams throughout the wavelength scan of the photolysis light, which may cause a horizontal walk-off of the laser beam position. Furthermore, in order to keep the securer spatial overlap for a long-range photolysis wavelength scan for the lowest energy peak at 157 nm exhibiting a structureless broad feature, the autotracking system for the LiF prism has been developed.[15]

The 148-nm fluorescence from the $S(^3D_1{}^o)$ in eq 3 was detected by a solar blind photomultiplier (Hamamatsu R1259) with LiF focusing lenses, located in the direction perpendicular both to the laser beams and to the free jet. The signal from the photomultipler was amplified by a preamplifier (NF BX-31) and averaged by a boxcar integrator (Stanford SR250). The intensities of the photolysis and the probe laser beams were monitored by a photomultiplier and by a photodiode, respectively, during the PHOFEX measurements for the normalization of the PHOFEX signal intensities.

The $A^1\Pi-X^1\Sigma^+$ (v', v'') transitions of CO were also measured for the wavelength calibration of the photolysis laser light. The rotational lines of the (v', v'') = (0, 0), (1, 0), and (2, 0) vibrational bands were used as frequency standards.[16] From the FWHM of the isolated rotational lines, the bandwidth of the vacuum UV laser was estimated to be 0.44(5) cm^{-1}. The rotational temperature of OCS in the free jet was estimated to be 5 K, which was obtained by fitting the intensity pattern of the rotational structure of the $A^1\Pi-X^1\Sigma^+$ transitions of CO, measured under the same expansion conditions.

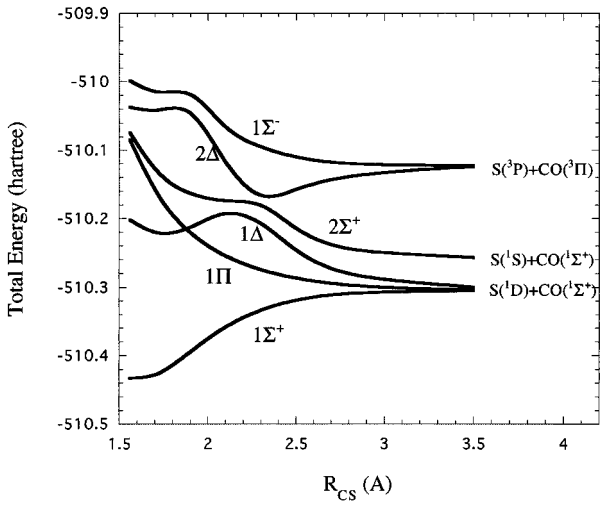

Figure 2. Shape of the CASSCF potentials for the low-lying singlet states of OCS as a function of the CS bond length ($R_{CO} = 1.16$ Å).

III. Theoretical Section

A. *Ab Initio* Potential Energy Surfaces. The PES's of low-lying singlet excited states of OCS were obtained by *ab initio* molecular orbital calculations. The complete active space self-consistent-field (CASSCF) method was used with the valence double-ζ-plus polarization (cc-pVDZ) basis set.[17] The present calculations were carried out with the MOLPRO suite of *ab initio* programs developed by Werner and Knowles.[18]

The electronic ground state of OCS has the Hartree−Fock configuration

$$...(6\sigma)^2(7\sigma)^2(8\sigma)^2(9\sigma)^2(2\pi)^4(3\pi)^4(4\pi)^0(10\sigma)^0(11\sigma)^0 \quad (1^1\Sigma^+)$$

For the CASSCF calculations, we have chosen 10 electrons and 9 orbitals (9σ, 2π, 3π, 4π, 10σ, 11σ) as the active space. Three Σ^+, two Δ, two Π, and one Σ^- states correlate with three low-lying asymptotes, $S(^3P) + CO(^3\Pi)$, $S(^1S) + CO(^1\Sigma^+)$, and $S(^1D) + CO(^1\Sigma^+)$. In order to obtain sufficiently accurate energies for these 8 low-lying electronic states, the 12 states (5 A_1, 2 B_1, 2 B_2, and 3 A_2 in C_{2v} symmetry) have been optimized in a state-averaged CASSCF procedure with equal weights.

Shown in Figure 2 are the potential curves of OCS obtained from the CASSCF method for the low-lying singlet states as a function of the C−S bond length (R_{CS}). The C−O distance (R_{CO}) was fixed at $R_{CO} = 1.16$ Å, i.e., the equilibrium C−O distance of the electronic ground state of OCS.[19] The first excited state was calculated to be the $^1\Delta$ state resulting from a $3\pi \rightarrow 4\pi$ excitation. This $^1\Delta$ state, $1^1\Delta$, was found to correlate adiabatically with $S(^1D) + CO(^1\Sigma^+)$ and diabatically with $S(^3P) + CO(^3\Pi)$ as the asymptotes. A strong avoided crossing between the $1^1\Delta$ state and the second lowest $^1\Delta$ state, $2^1\Delta$, forms a relatively deep well along the R_{CS} coordinate. The second lowest excited state, $1^1\Pi$, resulting from a $3\pi \rightarrow 10\sigma$ transition is repulsive and crosses with the $1^1\Delta$ state near $R_{CS} = 1.8$ Å. The $2\Sigma^+$ state resulting from a $3\pi \rightarrow 4\pi$ excitation was found to have the largest transition dipole moment from the electronic ground $1^1\Sigma^+$ state among the seven low-lying excited states and is primarily repulsive toward the $S(^1S) + CO(^1\Sigma^+)$ asymptote, with a characteristic shoulder at $R_{CS} \sim 2.3$ Å.

A total of 100 geometries were calculated and fitted to splines for wavepacket calculations. The contour plots of the 2D

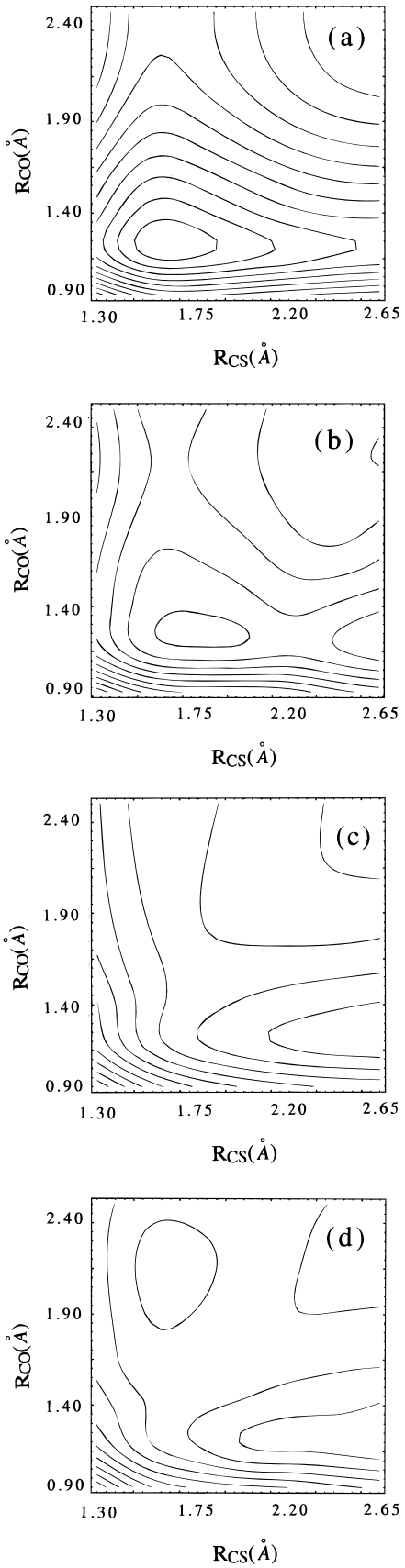

Figure 3. Contour plots of the CASSCF potential energy surfaces of OCS for the (a) $1^1\Sigma^+$, (b) $1^1\Delta$, (c) $1^1\Pi$, and (d) $2^1\Sigma^+$ states. Note that the bottom right end corresponds to the CO + S channel.

CASSCF PES's are given in Figure 3 for the four low-lying states; (a)$1^1\Sigma^+$, (b)$1^1\Delta$, (c)$2^1\Pi$, and (d)$2^1\Sigma^+$.

B. Wavepacket Propagation. The collinear OCS system was described by the Hamiltonian

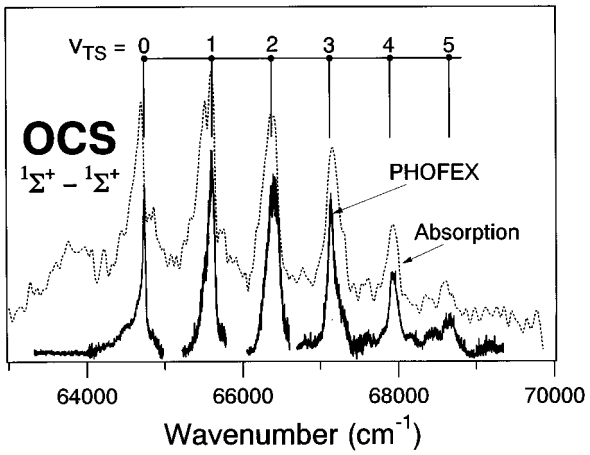

Figure 4. PHOFEX spectrum measured under jet-cooled conditions (lower trace, solid line) and the absorption spectrum measured by McCarthy and Vaida[12] (upper trace, dashed line) of the entire $^1\Sigma^+ - {}^1\Sigma^+$ transition of OCS in the 143−159-nm region. The relative intensities of the PHOFEX spectrum were normalized with respect to the absorption spectrum assuming that the backgroundlike features are originated mainly from the hot band transitions.

$$H = -\frac{\hbar^2}{2\mu_{CS}}\frac{\partial^2}{\partial R_{CS}^2} + \frac{\hbar^2}{2m_c}\frac{\partial^2}{\partial R_{CS}\partial R_{CO}} - \frac{\hbar^2}{2\mu_{CO}}\frac{\partial^2}{\partial R_{CO}^2} + V(R_{CS}, R_{CO}) \quad (4)$$

where μ_{CS} and μ_{CO} are the reduced masses of CS and CO, respectively, and m_C is the mass of a carbon atom. The wavepacket $\psi(R_{CS}, R_{CO}, t)$ was represented on a uniform 64 × 64 grid and propagated by using the Newtonian interpolation scheme[20] with a time step of 10.0 au. The initial wavepacket is obtained by the relaxation method[21] with an imaginary time propagation on the PES of the electronic ground $1^1\Sigma^+$ state.

IV. Results and Discussion

A. Overall Feature of the PHOFEX Spectrum. In Figure 4 is shown the PHOFEX spectrum measured in the present study by monitoring the S(^{1}S) fragments under jet-cooled conditions. The absorption spectrum of the jet-cooled OCS measured by McCarthy and Vaida[12] is also shown for comparison, which is obtained by reading points off of the enlarged copy of the published spectrum and by smoothly connecting them by a spline curve. Six distinct peaks with an almost equal spacing (≈800 cm^{-1}) are identified in both spectra, but the widths of the peaks in the PHOFEX spectrum, except the highest energy peak, are considerably narrower than the corresponding peaks in the absorption spectrum. The difference is most prominent for the lowest energy peak at 64 745 cm^{-1} in the PHOFEX spectrum, where the PHOFEX line width is only a quarter of the absorption peak width. The narrower features in the PHOFEX spectrum originated from the fact that the broadening due to the rotational and vibrational structure is largely decreased in the PHOFEX measurements and that the spectral resolution in the PHOFEX measurements, determined by the resolution of a tunable vacuum UV laser, is significantly high (∼0.5 cm^{-1}). Furthermore, the large backgroundlike feature with a broad peak around 63 870 cm^{-1} (or 156.6 nm) almost disappears in the PHOFEX spectrum. As will be discussed in section IV.B, this backgroundlike structure was assigned to hot band transitions. The intensities of the peaks in the PHOFEX spectrum shown in Figure 4 were normalized to the corresponding peaks in the absorption spectrum[12] whose intensities were derived by subtracting the underlying backgroundlike feature.

TABLE 1: Peak Positions and Widths for the Six Distinct Features[a] in the PHOFEX Spectrum of the $^1\Sigma^+-{}^1\Sigma^+$ Transition of Jet-Cooled OCS and Those in the Absorption Spectrum Reported by McCarthy and Vaida[12] (Results of the Fano Profile Analysis for the PHOFEX Spectrum Are Also Shown)

this work							ref 12	
				Fano profile analysis				
v_{TS}[b]	ν, cm^{-1}	Γ, cm^{-1}	τ, fs	E_r, cm^{-1}	Γ, cm^{-1}	q	ν, cm^{-1}	Γ,[c] cm^{-1}
0	64 745(2)	42(2)	133	64 750(3)	49(7)	−3.5(8)	64 704	156
1	65 605(5)	120(15)	44	65 608(5)	105(10)	−8.1(7)	65 561	224
2	66 392(15)	200(10)	27	66 402(7)	186(20)	−20(3)	66 347	223
3	67 134(8)	113(8)	47	67 129(5)	117(10)	9.3(7)	67 106	186
4	67 924(10)	121(8)	44	67 927(5)	119(10)	20(5)	67 906	167
5	68 644(20)						68 633	

[a] For the $v_{TS} = 5$ peak at 68 644 cm^{-1}, Γ and τ were not obtained, because the small neighboring bands on the lower energy side of this peak were expected to deform this peak to a certain extent. [b] The resonance vibrational quantum numbers of the in-phase stretching mode in the transition-state region in the excited $^1\Sigma^+$ state. [c] Derived from an enlarged copy of the published spectrum of the jet-cooled OCS.[12]

The stagnation-pressure dependence of the peak profile at 64 745 cm^{-1} in the PHOFEX spectrum was investigated in detail at stagnation pressures ranging between 0.3 and 3 atm. At pressures below 1 atm, a weak broad feature is observed at the lower energy side separated 100 cm^{-1} from the main peak at 64 745 cm^{-1}. At the higher stagnation pressure, this weak feature, possibly due to a hot band transition, disappeared and no further change was detected in the band profile. An effect of clustering of OCS molecules on the absorption spectra[12] as well as on the photodissociation products[22] was discussed in previous studies. McCarthy and Vaida[12] observed a broadening of the peak width in the $^1\Sigma^+-{}^1\Sigma^+$ absorption spectrum and found that the relative intensity of the broad feature at 63 870 cm^{-1} with respect to the peak at 64 745 cm^{-1} increases as the stagnation pressure increases. This intensity increase of the broad feature was ascribed to the formation of $(OCS)_n$ clusters. However, in our measurements of the PHOFEX spectrum, no significant change was identified when the stagnation pressure was varied between 1 and 3 atm. Therefore, the influence of clustering should be negligibly small under our experimental conditions.

The band-head positions and the line widths of the PHOFEX and absorption spectra[12] are listed in Table 1. The band-head positions obtained from the absorption spectra by McCarthy and Vaida[12] are substantially shifted to lower wavenumbers from the PHOFEX data by 11−45 cm^{-1}. These large deviations would be attributed either to the wavenumber calibration in the absorption measurements or to the contribution from the hot band transitions in the absorption spectrum, which may shift the top positions of the six main peaks.

Due to sufficient vibrational and rotational cooling in the supersonic jet and to the significantly high resolution (∼0.5 cm^{-1}) of the photolysis laser, the band profiles of the PHOFEX spectrum are expected to directly reflect the dissociation dynamics on the upper electronic state PES. Indeed, the broadening due to the rotational distribution was estimated to be at most ∼1.0 cm^{-1} for all six peaks from the rotational simulation at 5 K using the rotational constant of the electronic ground state[23] ($B'' = 0.2029$ cm^{-1}). Since the resolution of the photolysis laser is 0.44(5) cm^{-1}, the homogeneous line widths were derived by subtracting the rotational broadening and the laser resolution from the observed full widths at half-maximum (fwhm), Γ.

It can also be noticed in Figure 4 that the widths of the six main peaks exhibit characteristic variations. The observed line widths and the corresponding dissociation lifetimes of the main peaks in the PHOFEX spectra are listed in Table 1. From the lowest energy member of the six main peaks at 64 745 cm^{-1} to the third lowest peak, the peak width increases as the energy increases, but further excitation to the higher vibrational peaks leads to a certain reduction of the peak width, reflecting qualitative difference in the dissociation dynamics in the lower and higher energy regions on the upper $^1\Sigma^+$ PES.

Another important feature identified in the PHOFEX spectrum is asymmetric peak profiles for the six main peaks. As will be discussed in section IV.D, this asymmetry in a peak profile, known as a Fano profile,[24] was interpreted as a quantum interference effect between zero-order discrete and continuum states. Furthermore, it is clearly seen, in the profiles for the five low-lying members of the main peaks, that the shading toward the lower and higher energy sides was observed for the two low-lying and two high-lying peaks, respectively, and a nearly symmetrical profile was observed for the center peak. Such a change in the asymmetry direction in a Fano profile is known as *q reversal*.[25]

B. Assignments of Vibrational Resonances at the Transition State. Previous researchers[7,12] have reached an agreement that the six main peaks observed between 64 500 and 69 000 cm^{-1} can be attributed to the $^1\Sigma^+-{}^1\Sigma^+$ transition. However, assignment of the broad feature in the lower energy side at 63 870 cm^{-1} (156.6 nm) has not been established. Rabalais *et al.*[7] assigned this broad feature at 157 nm to a part of the $^1\Sigma^+-{}^1\Sigma^+$ transition, while McCarthy and Vaida[12] suggested that the broad feature is due to the transition to a bent $^1\Pi$ state on the basis of the absorption spectrum of jet-cooled OCS. On the one hand, Strauss *et al.* photolyzed OCS at 157 nm and showed that the transition is a parallel type based on the anisotropy of the spatial distribution of S and CO fragments.[26]

As clearly seen in Figure 4, the broad feature at 63 870 cm^{-1} observed in the absorption spectrum[12] almost disappears in the PHOFEX spectrum. Since the absolute quantum yield of the S(^{1}S) fragments was derived to be 0.8−1.0 in the 157-nm region,[14] the intensity decrease in the PHOFEX spectrum cannot be ascribed to the existence of a different dissociation channel. In our PHOFEX measurements, a very low rotational temperature (∼5 K) was achieved when OCS (7%)/Ar was expanded with 1.5 atm of stagnation pressure. On the other hand, McCarthy and Vaida[12] measured the absorption spectrum under jet-cooled conditions using OCS (10%)/N_2 with a stagnation pressure of 100 Torr. It is probable that the vibrational temperature for the absorption spectrum measured by McCarthy and Vaida was considerably higher than ours. Therefore, our observation, in which the broad feature at 157 nm in the absorption spectrum almost disappeared, indicates that this broad feature can be attributed to a hot band transition from vibrationally excited level in the electronic ground $^1\Sigma^+$ state. Since the energy spacing 875 cm^{-1} between the center of this broad feature and the neighboring sharp peak at 64 745 cm^{-1} is close to the vibrational frequency of the CS stretching motion in the ground state,[23] 859 cm^{-1}, the broad feature was assigned to a hot band transition from the first vibrationally excited state in the CS stretching mode ($v''_{CS} = 1$). In the PHOFEX spectrum,

the background feature covering the entire absorption spectrum almost disappears. This backgroundlike feature is also ascribed to the hot band transitions, possibly from the same $v''_{CS} = 1$ level or from the low-lying bending excited levels in the electronic ground state.

The vibrational frequency of the CS stretching mode, v_{CS}, in the electronic ground state is $v_{CS} = 858.9$ cm^{-1} so that the relative population of the $v''_{CS} = 1$ level is only 2% of the vibrational ground level even under room-temperature conditions. Thus, a relatively large contribution of this hot band transition in the absorption spectrum implies that the Franck−Condon factor from the $v''_{CS} = 1$ vibrationally excited level in the electronic ground $^1\Sigma^+$ state to the excited $^1\Sigma^+$ state should be significantly large. Therefore, it may be necessary to consider the substantial contribution from the vibrationally excited OCS for the proper modeling of the sulfur cycle in the stratosphere.[27]

Since a broad feature at 63 870 cm^{-1} was attributed to the hot band transition, the sharp peak at 64 745 cm^{-1} (154.5 nm) was assigned to the electronic band origin of the $^1\Sigma^+ - ^1\Sigma^+$ transition of OCS. In the previous study,[12] the distinct vibrational progression with a spacing of about 800 cm^{-1} for the $^1\Sigma^+ - ^1\Sigma^+$ band was assigned to the transitions to the CS stretching excited levels in the upper $^1\Sigma^+$ state based on the fact that the fundamental wavenumber for the CS stretching in the electronic ground state,[23] $v_{CS} = 858.9$ cm^{-1}, is similar to the spacings. On the other hand, it is known that the excitation to the upper $^1\Sigma^+$ state leads to only one dominant dissociation channel[14] of CO($X^1\Sigma^+$) + S(^{1}S), in which the C−S bond is broken. Since the dissociation occurs very fast in the femtosecond time scale as shown in Table 1, the PES of the excited $^1\Sigma^+$ state is expected to be mostly repulsive along this dissociation coordinate. Therefore, this distinct progression should not be assigned to the CS stretch motion along the dissociation coordinate. A spectral structure for a dissociating state can reflect the vibrational motion orthogonal to the reaction coordinate in the transition-state region. This vibrational motion near the transition-state region was characterized using the *ab initio* PES as described below.

As seen in Figure 3d, the *ab initio* PES of the excited $^1\Sigma^+$ state is dissociative along the CS stretching coordinate, while it is bound along the C−O bond distance with a broad plain along the CO stretching coordinate. The time evolution of the wavepacket on the upper $^1\Sigma^+$-state PES is depicted in Figure 5, as three snapshots. At $t = 0$, the initial wavepacket was prepared at the Frank−Condon region from the electronic ground state. It is clearly demonstrated in these figures that a part of the wavepacket evolves along the dissociation coordinate fairly rapidly, while the other part of the wavepacket remains near the Franck−Condon region for a certain period of vibration and moves along the *in-phase* stretching coordinate with comparable vibrational amplitudes for both CO and CS stretching motions. This motion of the wavepacket is expected to afford the prominent spectral peaks in the $^1\Sigma^+ - ^1\Sigma^+$ transition. The present wavepacket calculation confirms the above argument that the prominent progression represents the transition-state vibrational motion in the direction perpendicular to the dissociation coordinate and indicates that the vibrational mode is the in-phase stretching mode. Hereafter, this in-phase stretching vibrational mode at the transition state is referred to as the *transition-state vibrational mode* and its associated resonance vibrational quantum number is denoted as v_{TS}. This vibrational motion can be regarded as that along an unstable periodic orbit on the excited $^1\Sigma^+$ PES.

Besides the six main peaks, weak features are visible in the PHOFEX spectra at 66 790, 67 605, and 68 421 cm^{-1}. Mc-

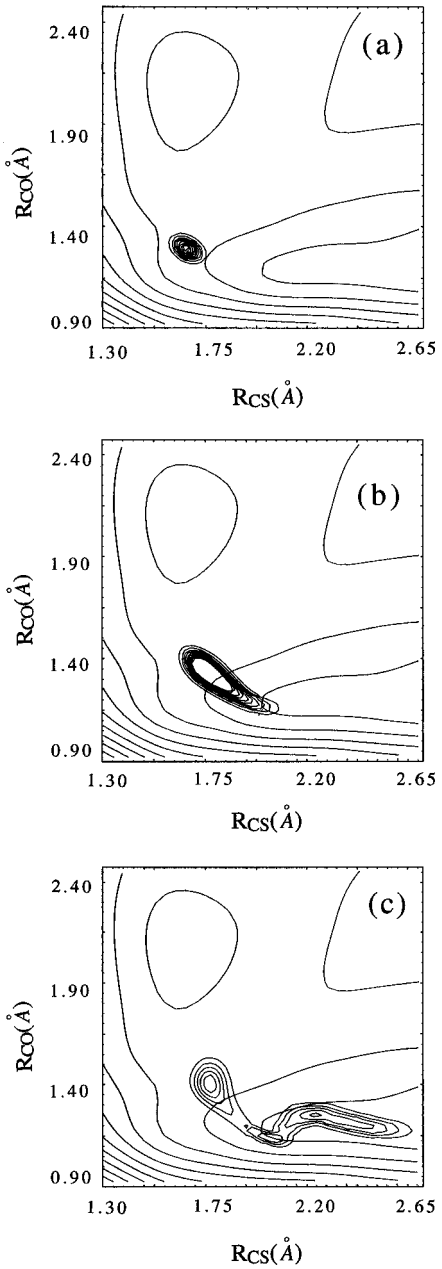

Figure 5. Time evolution of the dissociating wavepacket on the electronically excited Σ^+ state, $2^1\Sigma^+$, of OCS: (a) the initial wavepacket placed at the Franck−Condon region at $t = 0$ au and its snapshots at (b) $t = 500$ au (12 fs) and (c) $t = 1000$ au (24 fs).

Carthy and Vaida[12] also observed these weak features in the absorption spectra and assigned them to the progression in the CS stretching mode built on one quantum of the CO stretching mode in the upper electronic state. However, as discussed above, the main progression is due to the in-phase transition-state stretching mode, and the PES of the excited $^1\Sigma^+$ state is expected to be mostly repulsive along this dissociation coordinate so that the previous assignment is not appropriate. Instead, the progression is assigned to the in-phase transition-state stretching mode built on one quantum of the *bending* mode with a frequency of ca. 450 cm^{-1} in the upper electronic state. Therefore, the peaks found in the spectra at 66 790, 67 605, and 68 421 cm^{-1} may be assigned to the transition to the (v_{TS}, v'_{bend}) = (2, 1), (3, 1), and (4, 1) vibrational levels, respectively, where v'_{bend} denotes the vibrational quantum number of the bending modes in the upper $^1\Sigma^+$ state. The vibrational frequency for the bending mode v'_{bend} was thus calculated to be $v'_{bend} =$ 398, 471, and 526 cm^{-1} for $v_{TS} = 2$, 3, and 4, respectively. Since both of the two $^1\Sigma^+$ electronic states involved in the

electronic transition are known to have linear geometries at their equilibrium, weak intensities for the transitions to the bending excited state as seen in the spectra seems reasonable. The transitions to the lower vibrational levels (v_{TS}, v'_{bend}) = (0, 1) and (1, 1) are not clearly visible in the absorption spectra,[12] partly because of the overlap from the continuum-like background in the absorption spectrum, and also possibly because of their less favorable Franck−Condon factors. Unfortunately, due to a limited tunability of the dye lasers used to generate the vacuum UV photolysis laser light, the present PHOFEX spectrum does not cover the narrow energy regions where the transitions to the (v_{TS}, v'_{bend}) = (0, 1) and (1, 1) vibrational levels were expected to be observed. On the other hand, the three weak features may be ascribed to the transitions to the predissociative vibrational levels weakly trapped by a small potential hump along the dissociation coordinate, as in the case of FNO.[28] However, in order to perform secure assignments for these weak features, a more accurate PES of the excited $^1\Sigma^+$ state would be necessary, which will be derived by incorporating dynamical electron correlations.[29]

C. Femtosecond Transition-State Dynamics in the Excited $^1\Sigma^+$ State. An electronic absorption spectrum of molecules is closely related to the dynamics of the wavepacket representing nuclear motion on the upper electronic potential energy surface. The absorption spectrum, i.e., the absorption cross section $\sigma(E)$ as a function of an excitation energy E, and the motion of the wavepacket on the upper PES are related to each other by the Fourier transformation in the following formula:[3]

$$\sigma(E) \propto \int_{-\infty}^{+\infty} e^{iEt/\hbar} S(t)\, dt \quad (5)$$

$$S(t) = \langle \Phi(t) | \Phi(0) \rangle \quad (6)$$

where $\Phi(0)$ is the initial wavepacket prepared in the Frank−Condon region on the upper PES, and $\Phi_f(t)$ is the wavepacket at time t. The Fourier transform analysis of an absorption spectrum has been applied to various molecules such as O_3,[5,6] H_2O,[30,31] and H_2S[30] to discuss their photodissociation dynamics on the excited-state PES.

Previously, we reported[9] the Fourier transform analysis of the jet-cooled absorption spectrum of the $^1\Sigma^+-^1\Sigma^+$ band of OCS recorded by McCarthy and Vaida.[12] In the autocorrelation function in the time domain, a distinct peak was found at 41 fs, which was regarded as a period of the vibrational motion in the transition-state region along a classical unstable periodic orbit. However, as pointed out in section IV.A, the absorption spectrum suffers from vibrational and rotational congestion, though it was measured under jet-cooled conditions. Therefore, the results of the Fourier transformation may have been contaminated by the contribution from vibrational hot bands and rotational broadening. In order to derive the simplest dynamical information of OCS in its excited $^1\Sigma^+$ state, starting from the vibrational ground state of the electronic ground state, it is necessary to perform a Fourier transform analysis of an absorption spectrum measured under sufficiently cold conditions in vibrational and rotational degrees of freedom. Because the absolute quantum yield (0.8−1.0) of the S(^{1}S) photofragments is close to unity in the entire $^1\Sigma^+-^1\Sigma^+$ band of OCS, the PHOFEX spectrum obtained by monitoring S(^{1}S) should be almost identical to the absorption spectrum. Since the present PHOFEX spectrum is almost free from the influence of vibrational hot bands and rotational broadening, a Fourier transformation of the PHOFEX spectrum would afford clearer information on the dynamical behavior on the excited $^1\Sigma^+$ PES.

The Fourier transform of the PHOFEX spectrum is shown in Figure 6. The figure in the inset is the PHOFEX spectrum used in the analysis, which was constructed by connecting the adjacent PHOFEX peaks smoothly by a spline. Although there is some arbitrariness in determining the relative intensity of the PHOFEX peaks, it turned out that such uncertainty in the intensity has little influence on the main features in the resultant autocorrelation function. The first prominent recurrence observed in the autocorrelation function is at t = 42 fs, followed by the second recurrence at t = 83 fs. The third- and higher-order recurrences are also identified with detectable intensities. This long-lasting series of recurrences indicates that the wavepacket placed in the Frank−Condon region on the excited $^1\Sigma^+$ PES is trapped for a relatively long time in the vicinity of an unstable periodic orbit, whose direction is perpendicular to the dissociation coordinate. The period of 42 fs observed here corresponds to a vibrational frequency of 794 cm^{-1}, which reflects the interval (∼800 cm^{-1}) for the adjacent main features in the PHOFEX spectrum assigned as a progression for the in-phase transition-state stretching mode. A wavepacket calculation on the *ab initio* PES derived in the present study reproduced qualitative features of the experimental autocorrelation function, and a recurrence period of the 48 fs was obtained, which is comparable with the experimental value, 42 fs. This good agreement between experimental and theoretical vibrational periods in the transition-state region supports the fact that the present *ab initio* calculation reproduces an overall feature of the PES near the transition-state region.

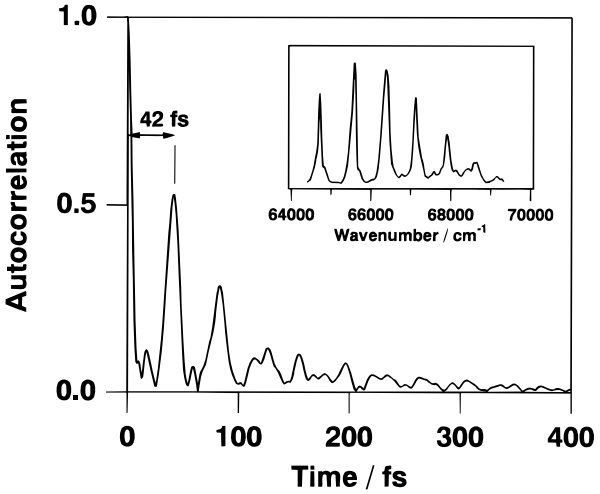

Figure 6. Autocorrelation function obtained from the Fourier transform of the PHOFEX spectrum of the entire $^1\Sigma^+-^1\Sigma^+$ transition of OCS. The PHOFEX spectrum is shown in the inset of the figure, which is derived by smoothly connecting the six experimental PHOFEX spectra by a spline. A clear series of recurrence is observed at t = 42, 83, and 127 fs and so on, which are essentially attributed to the in-phase stretching motion at the transition state of the upper $^1\Sigma^+$ state. Other recurrences may reflect a small contribution from the bending motion.

As listed in Table 1, the lifetimes of the five Feshbach-resonance vibrational levels for v_{TS} = 0−4 in the excited $^1\Sigma^+$ state were estimated from their homogeneous bandwidths, which were obtained by subtracting the laser resolution and the rotational bandwidth from the observed peak widths. As a peak width, a full width at half-maximum (FWHM) was adopted for the five broadened peaks. It should be noted here that a lifetime in the exact sense cannot be defined when a line shape is asymmetrical, which means that the decay process is not described as a single exponential. Therefore, the lifetimes derived here may be regarded as approximate estimates. Since it was difficult to determine the bandwidth of the sixth peak (v_{TS} = 5) in the progression due to an overlap with the other nearby weak features located on its lower energy side, the peak width and the lifetime of this peak were not derived.

A state-specific behavior of the transition-state vibrational levels in the excited $^1\Sigma^+$ state is clearly visible both in Figure

4 and in Table 1. The $\upsilon_{TS} = 0$ vibrational level, exhibiting the narrowest sharp profile, has a lifetime of $\tau(\upsilon_{TS}) = \tau(0) = 133$ fs, which corresponds to about 3 times the oscillation period, 42 fs, in the transition-state region, indicating that the dissociating OCS is able to oscillate back and forth for about 3 times in the transition-state vibrational mode prior to the complete dissociation. On the other hand, in the next higher lying peak, i.e., the transition to the $\upsilon_{TS} = 1$ level, OCS vibrates only once, since its lifetime was estimated to be $\tau(1) = 44$ fs. In the broadest peak, i.e., the transition to $\upsilon_{TS} = 2$, OCS almost instantaneously evolves into the dissociation coordinate, since $\tau(2) = 27$ fs is even shorter than one period of the in-phase transition-state stretching vibrational mode.

The above discussion on the acceleration of the dissociation rate for the higher lying PHOFEX peaks was also made in our previous work[11] on the basis of the peak broadening and the Fourier transform of the absorption spectrum measured by McCarthy and Vaida.[12] Until our present study, in which the jet-cooled PHOFEX spectrum for the entire $^1\Sigma^+ - ^1\Sigma^+$ transition was recorded, it was uncertain whether this tendency of the shorter lifetime for the higher lying PHOFEX peaks continues in the much higher energy region. One of the interesting findings in the present study for the higher energy region is that the homogeneous broadening was suppressed for the transitions to the $\upsilon_{TS} = 3$ and 4 levels so that the lifetimes become longer than that of the $\upsilon_{TS} = 2$ level. This deceleration of the dissociation for the quasi-bound levels in the higher energy than the $\upsilon_{TS} = 2$ level may be interpreted as the result of spatial extension of the vibrational wave function along the transition-state vibrational coordinate on the upper-state PES, which leads to an enhancement of a temporary trap of the wavepacket, resisting the motion along the dissociation coordinate. In fact, as shown in Figure 3d, the theoretical PES of the excited $^1\Sigma^+$ state has a shallow and broad plain toward the in-phase transition-state vibrational coordinate and the CO stretching coordinate, which would suppress the direct dissociation when a significant amount of the wave function is distributed in this region. This trapping of a wave function may result in longer lifetimes and, as a consequence, the narrower line widths for the large υ_{TS} ($\upsilon_{TS} \geq 3$) levels.

This narrowing of the bandwidth of the main progression at higher excitation energy may also be qualitatively explain by an adiabatic, time-independent picture, introduced by Schinke and co-workers[32] to interpret the photodissociation of FNO(n^*) $\rightarrow$ F + NO(n). Here n^* and n are the vibrational quantum numbers in the transition state of excited FNO and that in the ground state of NO.[32] In their treatment, the one-dimensional, vibrationally adiabatic potential curves, for which $n^* = n$, were calculated by assuming that motion along the dissociation coordinate is separable from the NO vibrational mode. The derived adiabatic potentials, which were primarily repulsive along the dissociation coordinate, were modified by the adiabatic correction term incorporating the coupling between the NO vibration and the dissociation. The correction term was found to be large near the transition-state region and form a barrier. This "dynamical barrier" becomes higher and wider as the vibrational quantum number, n, increases and, then, lengthens the dissociation lifetime. A similar interpretation may be applied to the photodissociation of OCS. When the dissociation dynamics of OCS is projected onto the one-dimensional motion and is modified by an adiabatic correction, the potential curve along the dissociation coordinate may become shallow, or even form a barrier, resulting in the deceleration of the dissociation rates for the higher lying vibrational states.

D. Asymmetric Profile and *q* Reversal in PHOFEX Spectra. *Observed Asymmetry in PHOFEX Spectra.* As mentioned in section IV.A, the prominent five peaks in the PHOFEX spectrum exhibit asymmetric peak profiles. The degree of asymmetry, i.e., an extent of deviation from a symmetrical Lorentzian line shape, decreases gradually from the lowest energy $\upsilon_{TS} = 0$ peak toward the $\upsilon_{TS} = 1$, 2 peaks, and then, the direction of the asymmetry is reversed in the $\upsilon_{TS} = 3$ and 4 peaks. In the present section, (i) the characteristic asymmetric peak profiles are interpreted as a result of a quantum interference effect between zero-order discrete and continuum states, (ii) the observed degree of asymmetry in the PHOFEX peaks is evaluated by a q parameter, which has been used to represent a Fano-type asymmetric profile, and (iii) a change in the asymmetry from the shading to the lower energy side for the three low-lying PHOFEX peaks to the shading to the higher energy side for the two high-lying peaks is interpreted as a phenomenon called q reversal.

In general, when discussing the asymmetry in an observed peak profile, inhomogeneous contributions causing peak asymmetry, such as the rotational band structure and an accidental overlap of the other transition peaks, should be carefully examined. In the PHOFEX spectrum, the contribution from the rotational structure can be neglected since the rotational bandwidth, reflecting the rotational population of the electronic ground $^1\Sigma^+$ state, is less than $\sim$1.0 cm^{-1} under jet-cooled ($T_R = 5$ K) conditions, which is considerably smaller than the PHOFEX peak widths (40$-$200 cm^{-1}). Concerning the second contribution, there could be two types of transitions overlapping with the main progression: (1) transitions to the other vibrational levels in the upper state and (2) hot band transitions from the vibrationally excited level in the electronic ground state.

However, these contributions are expected to be negligibly small from the following two reasons: Firstly, in the transition-state region, there could be 3 degrees of freedom in the vibrational motion, namely, (i) the transition-state vibrational mode, i.e., the in-phase stretching mode, whose direction is perpendicular to the dissociation coordinate, (ii) the $\angle$O$-$C$-$S bending mode, and (iii) the motion along the dissociation coordinate. The main progression was interpreted as the transitions to vibrational motion i, i.e., the transition-state vibrational levels. Since the PES of the upper $^1\Sigma^+$ state is mostly repulsive along the dissociation coordinate, as discussed in section IV.B., a contribution from the vibrational motion along dissociation coordinate iii to the PHOFEX spectrum may not be expected. Thus, the only vibrational mode that can possibly exhibit spectral features which could overlap the main features in the progression is the bending mode in the upper $^1\Sigma^+$ state. As mentioned in section IV.B, the vibrational frequency of the bending mode in the upper $^1\Sigma^+$ state could be roughly one-half of the frequency of the transition-state in-phase stretching mode, $\nu_{bend} \approx \nu_{TS}/2$ ($\sim$400 cm^{-1}). Therefore, the transitions to the second vibrational excited, $\upsilon'_{bend} = 2$, level in this bending mode can accidentally overlap the main progression. However, the transition-state vibrational progression built on the $\upsilon'_{bend} = 1$ vibrational level has a significantly weaker intensity than the main features, because of unfavorable Franck$-$Condon factors for the transitions from the linear $^1\Sigma^+$ ground state to the linear $^1\Sigma^+$ upper state. Therefore, the progressions built on two or more quanta in the bending mode are expected to have much smaller Franck$-$Condon factors so that they would have little influence on the shape of the main features.

Secondly, since the vibrational frequency of the CS stretching mode in the electronic ground state,[23] $\upsilon''_{cs} = 858.9$ cm^{-1}, is close to the spacing of the main progression in the $^1\Sigma^+ - ^1\Sigma^+$ transition, the overlap with the hot band transition from the $\upsilon''_{CS} = 1$ vibrational level can distort the profile of the main peaks. However, as discussed in section IV.B, because of sufficient

vibrational cooling in a supersonic jet under our experimental conditions, such hot-band transitions from the $v''_{CS} = 1$ vibrational level are suppressed considerably. In fact, the large backgroundlike structure as well as the feature at 63 870 cm^{-1} due probably to the hot band transition from the $v''_{CS} = 1$ vibrational level almost completely disappeared in the PHOFEX spectrum. Therefore, the asymmetric peak profiles in the PHOFEX spectrum could be explained only by the quantum interference effect.

Fano Profiles in Spectroscopy. Asymmetric line profiles, so-called Fano profiles, have often been observed in autoionization spectra of atoms and molecules, due to the interference between a discrete autoionizing level and ionization continuum. Fano[24] showed that the absorption spectrum $\sigma(E)$ in such a system exhibits an asymmetric profile given by the following formula using an asymmetry parameter q as

$$\sigma(E) = \sigma_0 \frac{(q+\epsilon)^2}{1+\epsilon^2} + \sigma_b \tag{7}$$

where $\epsilon = (E - E_r)/(\Gamma/2)$ is the dimensionless energy offset from the peak center E_r, and σ_0 and σ_b are the absorption cross sections to the continua, which are relevant and irrelevant to the interference effect, respectively. The asymmetric parameter q is a measure representing the coupling strength between the zero-order discrete and continuum states and is defined in terms of a zero-order discrete autoionizing state, ψ_d, and a zero-order continuum ionization state, ψ_c, both of which have non-zero transition moments from the common lower state, ψ_0, as

$$q = \frac{1}{\pi} \frac{\langle \psi_d|\mu|\psi_0\rangle}{\langle \psi_c|\mu|\psi_0\rangle\langle \psi_d|H_{dc}|\psi_c\rangle} \tag{8}$$

where H_{dc} is the interaction Hamiltonian between the zero-order discrete and continuum states and μ is the transition moment. Positive and negative values of q result in peak profiles shaded toward the higher and lower energy sides, respectively. When the absolute value of q is small, the degree of asymmetry is large, and when it becomes large, the line profile approaches a symmetrical Lorentzian profile.

Asymmetric line profiles were also found in predissociating diatomic molecules such as H_2,[33] O_2,[34] Cs_2,[35] and HgNe.[36] In the case of the dissociation of diatomic molecules, asymmetry in a peak profile is caused by a coupling between a zero-order bound state and a zero-order dissociation continuum. As has been discussed by Okunishi *et al.*,[36] a characteristic asymmetric line profile observed in the transitions to the lowest Rydberg state of HgNe can be classified into the *shape resonance*, since the dissociation occurs on a single electronic potential curve, while those found in H_2,[33] O_2,[34] and Cs_2[35] can be classified as the *Feshbach resonance*,[37] in which a zero-order bound state couples with a continuum state of a different electronic state.

For the dissociation of diatomic molecules, the q parameter in eq 8 is expressed by assuming that μ is independent of the nuclear coordinates[38] as

$$q = \frac{1}{\pi} \frac{\langle \phi_d|\mu|\phi_0\rangle\langle \chi_d|\chi_0\rangle}{\langle \phi_c|\mu|\phi_0\rangle\langle \chi_c|\chi_0\rangle} \frac{1}{\langle \phi_d\chi_d|H_{dc}|\phi_c\chi_c\rangle} \tag{9}$$

where ϕ and χ are the electronic and nuclear parts of a zero-order basis wave function, respectively.

Asymmetric band profiles have also been observed in the spectra of predissociating triatomic molecules.[39,40] In the dissociation of triatomic molecules, two different types of resonances, i.e., the Feshbach and shape resonances, can cause an asymmetric peak profile, even when the dissociation takes place on a single adiabatic electronic PES. The asymmetric peak profiles of OCS observed in the present study, reflecting the dissociation on the electronically excited $^1\Sigma^+$ PES, are categorized into the Feshbach-type resonance, in which the in-phase stretching coordinate, resulting in a zero-order bound vibrational state, couples with the motion along the dissociation coordinate, forming a zero-order dissociative continuum state. On the other hand, if there exists a well along the dissociation coordinate, the asymmetric band profile may also be caused by a shape resonance similar to HgNe.[36]

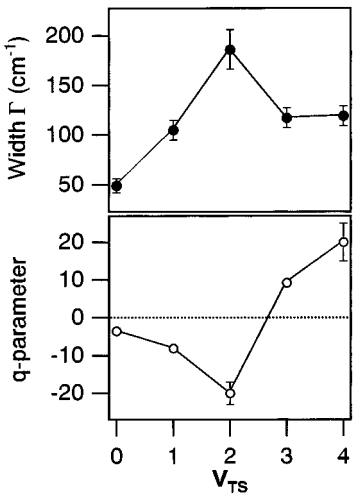

Figure 7. Width (Γ) and asymmetry (q) parameters derived from Fano profile analysis for the $v_{TS} = 0-4$ vibrational Feshback resonances in the present PHOFEX spectrum. A characteristic correlation betweeen Γ and q is clearly identified.

The vibrational Feshbach resonance on the excited $^1\Sigma^+$ PES of OCS clearly reflects the motion of the wavepacket shown in Figure 5, where the wavepacket prepared in the Franck-Condon region experiences a substantial bifurcation into the vibrating part staying near the transition-state region and the dissociative part extending toward a dissociation valley. It can be said that these two different types of nuclear motion interfere with each other and result in the vibrational Feshbach resonance affording asymmetric profiles. The asymmetrical absorption profiles in the dissociation of FNO[39] were also interpreted based on a wavepacket calculation by Cotting *et al.*[40] and were used to construct the upper-state PES by Shapiro and Reisler.[41]

q Reversal in OCS. The asymmetric band profiles observed in the PHOFEX spectrum were fitted to the Fano profile formula, eq 7, to measure the degree of asymmetry quantitatively. The results of the least-squares fit are summarized in Table 1, and the obtained width (Γ) and asymmetry (q) parameters are plotted as a function of v_{TS} in Figure 7. Since the five main peaks are energetically well separated in the PHOFEX spectrum of OCS, the fit was performed for individual peaks to determine the parameters E_r, q, and Γ. The fit was not performed for the sixth peak in the main progression, i.e., the $v_{TS} = 5$ band, because of the substantial overlap from the other nearby feature on the lower energy side as described in section IV.B. As shown in Table 1, the widths (Γ) determined by the Fano profile analysis are in good agreement with the FWHM of the peaks obtained in section IV.C. Sadeghi and Skodje[42] proposed an analytic line shape formula for asymmetric spectral peaks resulting from resonances in the transition-state region in the $D + H_2$ system. The formula was applied to the present PHOFEX spectra and provided an almost equally good fit as the Fano profile formula. However, the five parameters derived by fitting to the experimental spectra have clear physical meanings only for barrier resonances. Thus, we adopted here the conventional Fano profile formula, eq 7, for the discussion for the peak asymmetry.

The Fano profile analysis clearly showed that the bandwidth (Γ) and the asymmetric parameter (q) exhibit a characteristic correlation against the resonance vibrational quantum number, v_{TS}, as depicted in Figure 7. As v_{TS} increases, Γ increases and takes a maximum value at the $v_{TS} = 2$ peak and then decreases for the $v_{TS} = 3$ and 4 peaks, while q becomes negatively larger until the $v_{TS} = 2$ peak and, then, increases to take positive values for the $v_{TS} = 3$ and 4 peaks. This change of sign in the q parameter in a progression of the main absorption peaks has been known as a q-reversal phenomenon, observed often in autoionization spectra of atoms and molecules[25] and in the spectra of predissociating diatomic molecules.[35] The PHOFEX spectrum measured in the present study afforded a clear example in which the q reversal is observed for the dissociating *triatomic* molecules.

The multichannel quantum defect theory (MQDT)[43] showed that, in the autoionization spectra of atoms and molecules, the q-reversal phenomenon is caused by the presence of the third interloper state in addition to the two interacting discrete and continuum states. On the other hand, Kim *et al.*[35] observed the q reversal in the spectrum of predissociating Cs_2 molecules and mentioned that the q reversal can be observed even when only two electronic states exist, i.e., a bound state and a "structured" continuum state. As shown in eq 9, the asymmetry parameter q depends on the coupling matrix element between the discrete and continuum states, $\langle\phi_d\chi_d|H_{dc}|\phi_c\chi_c\rangle$. The q-reversal phenomenon observed in Cs_2 was ascribed to the crossing between the bound and continuum potentials at their outer limb, resulting in the oscillatory variations accompanying the sign change of the coupling matrix element $\langle\phi_d\chi_d|H_{dc}|\phi_c\chi_c\rangle$.

Since the dissociation is considered to proceed on a single electronic surface in the present OCS case, the q parameter may be expressed by setting $\phi_d = \phi_c$ in eq 9 as follows,

$$q = \frac{1}{\pi}\frac{\langle\chi_d|\chi_0\rangle}{\langle\chi_c|\chi_0\rangle}\frac{1}{\langle\chi_d|H_{dc}|\chi_c\rangle} \qquad (10)$$

As shown in eq 10, the value of asymmetric parameter q depends on three elements, i.e., (i) the coupling matrix element between the zero-order discrete and continuum states, $\langle\chi_d|H_{dc}|\chi_c\rangle$, (ii) the vibrational overlap integral between the zero-order discrete state χ_d and the vibrational ground state χ_0 in the electronic ground state, $\langle\chi_d|\chi_0\rangle$, (iii) the vibrational overlap integral between the zero-order continuum state χ_c and the vibrational ground state χ_0 in the electronic ground state, $\langle\chi_c|\chi_0\rangle$.

The q-reversal phenomenon observed in the PHOFEX spectrum of OCS can be explained in two different ways as described below. Since the dissociation of OCS in the excited $^1\Sigma^+$ state proceeds on the single electronic PES, the outer-limb crossing model adopted for Cs_2 cannot be applied for the present case. However, if the phase of the zero-order continuum wave function varies substantially in a narrow energy range, the q reversal would be caused as a result of the changes of the sign in the coupling element $\langle\chi_d|H_{dc}|\chi_c\rangle$, or in the vibrational overlap function, $\langle\chi_c|\chi_0\rangle$. In other words, the q reversal may be induced by another resonance mechanism, such as the shape resonance. If a small hump exists on the potential energy surface along the dissociation coordinate near the Franck−Condon region, it may cause a large phase shift in the continuum wave function χ_c, leading to the *q-reversal* phenomenon.

Alternatively, the q reversal may result from the changes in the sign of the overlap integral $\langle\chi_d|\chi_0\rangle$ between the zero-order discrete wave function, corresponding to the in-phase stretching vibrational motion at the transition state, and the vibrational ground state χ_0 in the electronic ground state. As the vibrational quantum number increases, the zero-order vibrational wave function is spatially extended toward the in-phase stretching or CO stretching coordinate as discussed in section IV.C, and substantial changes may occur in the nodal pattern of the zero-order vibrational wave function. Thus, the changes in the sign of the overlap integral, $\langle\chi_d|\chi_0\rangle$, may result in the q reversal. Although a definite conclusion on the origin of the observed q reversal in the spectrum of the dissociating OCS may not be drawn, the latter explanation is favored since there is a characteristic correlation between the v_{TS} dependence of the peak width and the q parameter as shown in Figure 7, and the dependence of the peak width on v_{TS} was interpreted by the trapping of the wave function in the transition-state region.

V. Summary

(1) The PHOFEX spectrum of the entire $^1\Sigma^+-{}^1\Sigma^+$ transition of OCS in the 63 300−69 350-cm^{-1} (144−158 nm) region was measured under jet-cooled conditions, by scanning the tunable coherent vacuum UV light and by monitoring the fragment S(^{1}S) atom. By sufficient vibrational and rotational cooling of OCS in a supersonic jet, the PHOFEX spectrum exhibiting a simplified vibrational structure with an average interval of ∼800 cm^{-1} was observed with almost no background structure. The five main peaks that are substantially narrower than in the previously recorded absorption spectra were regarded as those reflecting the ultrashort (27∼133 fs) transition-state dynamics with negligibly small vibrational and rotational inhomogeneity. Furthermore, the characteristic asymmetric peak profiles, which have been blurred in the previous absorption studies due to limited spectral resolution and to the overlapping vibrational and rotational structures, were extracted for the first time by the present high-resolution PHOFEX spectrum measured under ultracold conditions. In the autocorrelation function obtained from the Fourier transform of the observed PHOFEX spectrum, a vibrational period, 42 fs, characterizing the transition-state vibrational mode, was obtained.

(2) In order to identify the vibrational motion at the transition state with a 42-fs period, resulting in the observed characteristic vibrational progression, the *ab initio* potential energy surfaces of the electronic ground and excited $^1\Sigma^+$ states of OCS, as well as those of the excited $^1\Delta$ and $^1\Pi$ states, were calculated. The wavepacket calculation on the excited $^1\Sigma^+$ *ab initio* PES, having a shallow slope along the dissociation coordinate and a wide plateau region toward the CO stretching coordinate, was performed. The wavepacket exhibited an in-phase vibrational motion for the C−O and C−S bonds with a 48-fs period, which is orthogonal to the direction of dissociation. A good agreement between the experimental and theoretical vibrational periods supports the interpretation that the observed PHOFEX peaks represent the vibrational Feshbach resonance states in the transition-state region, in which the wavepacket is temporary trapped along the vibrational motion perpendicular to the dissociation coordinate, i.e., a so-called classical unstable periodic orbit. In other words, this simple and regular progression of the homogeneously broadened peaks with an average interval of ∼800 cm^{-1} was regarded as a pure progression of the transition-state vibrational mode. Based on this interpretation, the resonance states were assigned using the vibrational quantum number v_{TS} for the transition-state vibrational motion. It is also noteworthy that the broad feature at 63 870 cm^{-1} (∼157 nm), whose spectroscopic origin was discussed previously by several researchers, was assigned to the hot band transition from the $v''_{CS} = 1$ vibrationally excited level in the CS stretching mode in the electronic ground $^1\Sigma^+$ state on the basis of the present jet-cooled PHOFEX measurements. Consequently, the sharp peak at 64 745 cm^{-1} (∼154 nm) was assigned to the origin band of the $^1\Sigma^+-{}^1\Sigma^+$ transitions of the dissociating OCS.

(3) It was discussed in the present study that the characteristic dissociation dynamics is encoded in the width and the asymmetry of the absorption peak profiles. As the excitation energy increases, a peak width for the main progression of the transition-state Feshbach resonances increases until $v_{TS} = 2$ and decreases for higher lying resonances, i.e., $v_{TS} = 3$ and 4. This narrowing of the peak width, i.e., the lengthening of the lifetime in the high-lying resonances, was interpreted as a consequence of the trapping of the wavepacket in the in-phase stretching transition-state vibrational coordinate or in a broad plateau region extending toward the CO stretching coordinate. The characteristic asymmetric band profiles observed for all the main peaks in the PHOFEX spectra were regarded as a Fano-type line profile resulting from the Feshbach resonance, in which a zero-order discrete state of the vibrational motion along the transition-state vibrational coordinate and a zero-order continuum state representing the motion along the dissociation coordinate interfere with each other. This quantum interference effect is also confirmed in the short time dynamics of the wavepacket which is composed of two components, i.e., the part moving back and forth along the transition-state vibrational coordinate and that propagating directly toward the dissociation coordinate. Furthermore, an interesting *q*-reversal phenomenon was found in the asymmetric peak profiles. The change in the direction of the asymmetry of the profiles was interpreted as that caused by a phase shift of the dissociating wave function in the narrow energy region, reflecting the shape of the PES in the transition-state region.

(4) Finally, from the present study of photodissociation of OCS in the deep vacuum UV region, we gained detailed and rich information about the dissociation dynamics such as transition-state vibrational resonances, contained in a clear way in the PHOFEX spectrum. Therefore, in general, measurements of an absorption spectrum, or a spectrum corresponding with an absorption spectrum such as a PHOFEX spectrum, with high resolution under jet-cooled conditions will be a most naive and direct way to uncover the characteristic transition-state dynamics of photodissociating small polyatomic molecules. As demonstrated in the present study, theoretical supports such as wavepacket dynamical calculations are also crucial for a clearer understanding of the dissociation dynamics on the multidimensional dissociative PES.

Acknowledgment. The present work is partially supported by Grant-in-Aid from the Ministry of Education, Science, Sports and Culture (Nos. 04243105, 05237205, 05453016, 05453026, 06228206, 06239213, 07240101, and 07240106). S. L. acknowledges financial support from the Japanese Government (Monbusho) Scholarship.

References and Notes

(1) Zwail, A. H. *Femtochemistry*; World Scientific: Singapore, 1994.
(2) Schinke, R. *Photodissociation Dynamics*; Cambridge University: Cambridge, 1993.
(3) Heller, E. J. *Acc. Chem. Res.* **1981**, *14*, 368.
(4) Schinke, R.; Engel, V. *J. Chem. Phys.* **1990**, *92*, 3252.
(5) Johnson, B. R.; Kinsey, J. L. *Phys. Rev. Lett.* **1989**, *62*, 1607; *J. Chem. Phys.* **1989**, *91*, 7638.
(6) Yamashita, K.; Morokuma, K.; LeQuere, F.; Leforestier, C. *Chem. Phys. Lett.* **1992**, *191*, 515. Leforestier, C.; LeQuere, F.; Yamashita, K.; Morokuma, K. *J. Chem. Phys.* **1994**, *101*, 3806.
(7) Rabalais, J. W.; McDonald, J. M.; Scherr, V.; McGlynn, S. P. *Chem. Rev.* **1971**, *71*, 73.
(8) Pibel, C. D.; Ohde, K.; Yamanouchi, K. *J. Chem. Phys.* **1994**, *101*, 834.
(9) Yamanouchi, K.; Ohde, K.; Hishikawa, A.; Pibel, C. D. *Bull. Chem. Soc. Jpn.* **1995**, *68*, 2459.
(10) Ohde, K.; Hishikawa, A.; Yamanouchi, K. *J. Elect. Spec. Rel. Phenom.* **1996**, *79*, 433.
(11) Yamanouchi, K.; Ohde, K.; Hishikawa, A. *Adv. Chem. Phys.*, in press.
(12) McCarthy, M. I.; Vaida, V. *J. Phys. Chem.* **1988**, *92*, 5875.
(13) Yamanouchi, K.; Tsuchiya, S. *J. Phys. B* **1995**, *28*, 133.
(14) Black, G.; Sharpless, R. L.; Slanger, T. G.; Lorents, D. C. *J. Chem. Phys.* **1975**, *62*, 4274. Black, G.; Sharpless, R. L. *J. Chem. Phys.* **1979**, *70*, 5567.
(15) Itakura, R.; Hishikawa, A.; Yamanouchi, K. To be published.
(16) Tilford, S. G.; Simmons, J. D. *J. Phys. Chem. Ref. Data* **1972**, *1*, 147.
(17) Dunning, T. H., Jr. *J. Chem. Phys.* **1989**, *90*, 1007.
(18) MOLPRO is a package of *ab initio* programs written by H.-J. Werner and P. J. Knowles, with contributions from J. Almlof, R. D. Amos, M. J. O. Deegan, S. T. Elbert, C. Hampel, W. Meyer, K. Peterson, R. Pitzer, A. J. Stone, and P. R. Taylor.
(19) Morino, Y.; Nakagawa, T. *J. Mol. Spectros.* **1968**, *26*, 496.
(20) Kosloff, R. *Annu. Rev. Phys. Chem.* **1994**, *45*, 145.
(21) Kosloff, R.; TalEzer, H. *Chem. Phys. Lett.* **1986**, *127*, 223.
(22) Sivakumar, N.; Hall, G. E.; Houston, P. L.; Hepburn, J. W.; Burak, I. *J. Chem. Phys.* **1988**, *88*, 3692.
(23) Herzberg, G. *Molecular Spectra and Molecular Structure, Electronic Spectra and Electronic Structure of Polyatomic Molecules*; Van Nostrand: New York, 1966.
(24) Fano, U. *Phys. Rev.* **1961**, *124*, 1866.
(25) Connerade, J. P.; Lane, A. M. *J. Phys. B* **1987**, *20*, 1757.
(26) Strauss, C. E.; McBane, G. C.; Houston, P. L.; Burak, I.; Hepburn, J. W. *J. Chem. Phys.* **1989**, *90*, 5364.
(27) Wayne, R. P. *Chemistry of Atmospheres*; Oxford University: Oxford, 1991.
(28) Ogai, A.; Brandon, J.; Reisler, H.; Suter, H. U.; Huber, J. R.; von Dirke, M.; Schinke, R. *J. Chem. Phys.* **1992**, *96*, 6643.
(29) Yamashita, K. To be published.
(30) Henriksen, N. E.; Zhang, J.; Imre, D. G. *J. Chem. Phys.* **1989**, *89*, 5607.
(31) Butler, L. J. *Chem. Phys. Lett.* **1991**, *182*, 393.
(32) Suter, H. U.; Huber, J. R.; von Dirke, M.; Untch, A.; Schinke, R. *J. Chem. Phys.* **1992**, *96*, 6727.
(33) Siebbeles, L. D. A.; Schins, J. M.; Los, J.; Glass-Maujean, M. Phys. Rev. A. **1991**, *44*, 1583. Glass-Maujean, M.; Breton, J.; Guyon, P. M. *Chem. Phys. Lett.* **1979**, *63*, 591.
(34) Gibson, S. T.; Lewis, B. R. *J. Elect. Spec. Rel. Phenom.* **1996**, *80*, 9.
(35) Kim, B.; Yoshihara, K. *J. Chem. Phys.* **1993**, *99*, 1433. Kim, B.; Yoshihara, K.; Lee, S. *Phys. Rev. Lett.* **1994**, *73*, 424.
(36) Okunishi, M.; Yamanouchi, K.; Onda, K.; Tsuchiya, S. *J. Chem. Phys.* **1993**, *98*, 2675.
(37) Child, M. S. *Molecular Collision Theory*; Academic: London, 1974.
(38) Lefebvre-Brion, H.; Field, R. W. *Perturbations in the Spectra of Diatomic Molecules*; Academic: Orland, 1986.
(39) Brandon, J. T.; Reid, S. A.; Robie, D. C.; Reisler, H. *J. Chem. Phys.* **1992**, *97*, 5246. Reid, S. A.; Brandon, J. T.; Reisler, H. *J. Phys. Chem.* **1993**, *97*, 540.
(40) Cotting, R.; Huber, J. R.; Engel, V. *J. Chem. Phys.* **1994**, *100*, 1040.
(41) Shapiro, M.; Reisler, H. *J. Chem. Phys.* **1995**, *103*, 4150.
(42) Sadeghi, R.; Skodje, R. T. *J. Chem. Phys.* **1995**, *102*, 193.
(43) Giusti-Suzor, A.; Lefebvre-Brion, H. *Phys. Rev. A* **1984**, *30*, 3057.